

PSF Estimation based on Speckle Illumination

Sidy Ndiongue, Sarvath Sharma

Abstract—Optical imaging systems often face performance challenges due to imperfections in the point spread function (PSF), affecting resolution. In this project, we propose a computational optical technique using speckle-pattern illumination to correct aberrations without the need for adaptive optical elements, addressing acquisition and complexity issues. Speckle illumination, generated through light wave interference, offers a promising solution for diverse applications, including tissue imaging. Its inherent phase randomness effectively cancels out aberrations, serving as a natural reference pattern for precise PSF estimation and enhancing optical system quality.

I. INTRODUCTION

The point spread function (PSF) represents the response of an optical system to a point source of light. It characterizes how an idealized point source is transformed by the system, influencing the distribution of light in the final image. The PSF plays a pivotal role in determining the resolution and quality of an optical system. Imperfections in the PSF, often caused by inhomogeneities in the propagation medium or flaws in optical components, can lead to distortions and degradation in image quality. Strategies for addressing PSF imperfections include the use of adaptive optical elements or, as proposed in this study, computational optical techniques leveraging speckle-pattern illumination to achieve aberration correction for varying focal distances without additional complex optical elements.

As mentioned the use of speckle illumination can correct the aberrations caused by the optical elements in the system. Speckle illumination is a technique in optical imaging that harnesses random, granular patterns known as speckles, resulting from the interference of light waves [2]. In the context of imaging systems, speckle patterns are employed to mitigate the adverse effects of aberrations in optical systems. Unlike traditional methods relying on adaptive optics, speckle illumination offers a natural and computationally efficient approach to correcting aberrations without the need for additional adaptive optical elements. The inherent phase randomness of speckles plays a crucial role in canceling out aberrations present in the illumination path, serving as a spontaneous reference pattern for precisely estimating the PSF and improving the overall quality of optical systems.

II. RELATED WORK

Introduced in 2016, the PSF Estimation from Projected Speckle Illumination (PEPSI) technique offers a method for estimating the point spread function (PSF) of an imaging system [6]. The resolution of imaging systems is ideally limited by diffraction, but practical issues such as inhomogeneities in the light-propagating medium or optical imperfections often degrade image resolution. PEPSI utilizes the randomness of

speckle patterns to counteract aberrations in the illumination path, providing an objective pattern for assessing imaging path deformations. Notably, PEPSI allows for wide-field-of-view and local-PSF estimation without requiring calibration, achieved through a single speckle-pattern projection.

Hwang et al. [5] propose a method for imaging through turbulent media using short-exposure images. They recover the Fourier power spectrum of objects by applying Labeyrie's autocorrelation method and Fourier transforming its output, revealing that coherently averaging the images yields crucial Fourier phase information.

Premillieu et al. [7] utilize speckle illumination and gradient descent, combined with estimated shifted positions of an object, to recover the illumination and point spread function (PSF) of an optical system. An advantage of this approach is its independence from prior knowledge about the optical system. The resolution of the output is determined by the size of the speckles.

Similar to [5], Hwang et al. [4] employ speckle illumination but with sub-images, resulting in uncorrelated images. They extract the estimated PSF magnitude through power spectrum averaging and the estimated PSF phase through coherent averaging.

III. PROPOSED METHOD

A. PSF & MTF Theory

The Modulation Transfer Function (MTF) quantifies the ability of an imaging system to reproduce contrast variations in an object. It is defined as the ratio of the contrast in the image to the contrast in the object, as a function of spatial frequency. The MTF curve provides insights into the system's ability to transfer various spatial frequencies, with a higher MTF indicating better resolution.

The MTF equation is given by:

$$MTF(f) = \frac{|I(f)|}{|O(f)|} \quad (1)$$

where, $I(f)$ is the contrast of the image, $O(f)$ is the contrast of the object, and f is the spatial frequency of system. The MTF is often expressed as a normalized function ranging from 0 to 1, where 1 indicates perfect transfer of contrast [8].

The PSF describes the distribution of light intensity in the image resulting from a point source in the object space. The PSF is essentially the impulse response of the system and provides information about the spread of light over space [9]. The PSF can identify the spreading or blurring exhibited by a point object which serves as an indicator of the imaging system's quality. The PSF equation is given by:

$$I(x, y) = \int \int O(u, v)h(x - u, y - v)dudv \quad (2)$$

where $I(x, y)$ is the intensity distribution in the image, $O(u, v)$ is the object intensity distribution and $h(x, y)$ is the impulse response of the system or commonly known as the PSF.

If seen closely, it can be said that the PSF is the spatial domain version of the MTF. In other words, the relationship between MTF and PSF is established through the Fourier transform. The MTF is the modulus of the Fourier transform of the PSF, illustrating the system's frequency response. If we take the Fourier transform of the PSF and rearrange the terms we can see that,

$$MTF(f) = |\mathcal{F}\{h(x, y)\}| \quad (3)$$

Eqn-3 will help us identify and develop the simulations required for the stated application. In summary, the MTF quantifies the system's ability to transfer contrast at different spatial frequencies, while the PSF characterizes the spread of light in the image.

B. Speckle Patterns

Speckles can be identified as a form of random noise. They form when laser light interacts with rough surfaces, such as paper or a wall, and imprints a distinctive granular pattern with high contrast. The incident light of the laser is relatively uniform but as they hit the surface they leave a random intensity pattern fashioned by the mutual interference of a set of wavefronts having different phases [2]. For the speckles to be visible the coherence time needs to be relatively long. Most real-world materials exhibit roughness on the order of an optical wavelength, with exceptions like mirrors.

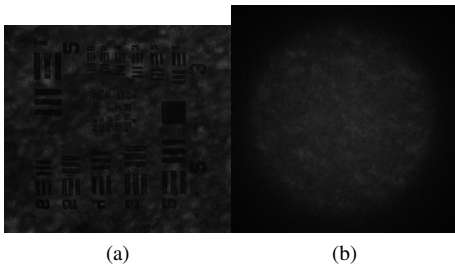


Fig. 1: Speckles on rough surfaces: (1a) Speckles on a US Air Force Target (USAF); (1b) Speckles on a tissue phantom

From Fig-1 it can be seen that for a laser source operating at 680nm a speckle pattern is formed on two different surfaces with their respective roughness. For the case of Fig-1a the laser has a diffuser in the path causing the production of random phases and thus an interference of a set of wavefronts leading to a "granular" pattern.

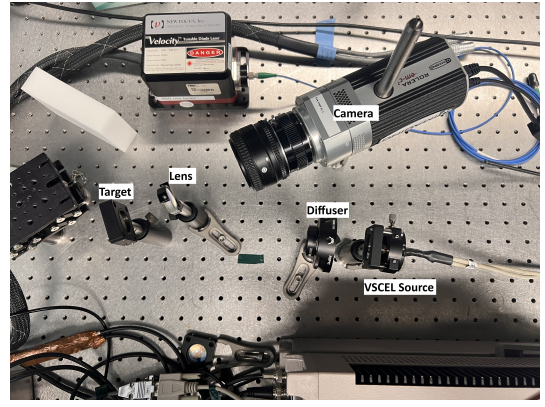


Fig. 2: Experimental Setup to obtain speckles on USAF target

Rolera EM-C ² CCD Camera (QImaging)	Pixel Size Sensor Size Resolution Field of View (FoV)	8x8mm 8x8μm 1002x1002 pixels 6x6 cm
Nikon Camera Lens	Focus Distance Focal Length Aperture Size	50 cm 50 mm f/16
ThorLabs Lens	Focal Length	50mm
VSCSEL Source	Wavelength	680nm
1" Diffuser	Grit	1500

TABLE I: Specifications of Optical Components

C. Experimental Setup

Fig-2 shows the attempted setup of the system to obtain speckle patterns on the USAF target. The components and their specifications are laid out in Fig-2 and Table-I.

Note the images were captured in the dark to ensure that there was enough light visible on the USAF target and that the camera did not pick up noise from the surrounding light. The diffuser used is on a rotating stage that will be rotated every 10° so that we can change the speckle pattern per defocus distance. This will allow for varying data points at each defocus stage and using those points we can develop a fine-tuned PSF. Along with the given specifications of the optical components we also ensured certain distances between the target and the camera. Since we want to avoid magnification from the camera to ensure we see the correct size of the speckles, we calculate the magnification of the imaging path for a region of interest (ROI):

$$\begin{aligned}
 M &= \frac{\text{Length of Desired Image}}{\text{Camera Length of Desired Image}} \\
 &= \frac{\frac{\text{Physical Size of Object}}{\text{Pixel Count of Object}} * \text{Pixel Count of ROI}}{\text{Camera Pixel Length of ROI} * \text{Camera Dimensions}} \\
 &= \frac{\frac{25400\mu m}{965.488px} * 20.524px}{72px * 8\mu m/px} \\
 &= \frac{576\mu m}{540\mu m} \approx 1.067
 \end{aligned} \quad (4)$$

Eqn-4 shows that we are using approximately a 1-1 magni-

fication system. Note that the diffraction-limited spot should be smaller/approximately the size of a pixel. Moving onto the next part is calculating the depth of focus (DOF). Our main goal is to estimate the PSF for varying fields of focus using speckle illumination. As we move the object within sections of the depth of field we expect the PSF to get larger since it gets more defocused and is imaged as larger circles rather than points.

$$\text{Depth of Field (DOF)} = \frac{2cs^2}{fN^2}$$

where:

- DOF is the depth of field,
 - c is the circle of confusion,
 - s is the subject distance,
 - f is the f-number (aperture),
 - N is the f-stop number (aperture diameter).
- (5)

$$c = \frac{\text{diagonal of sensor size}}{1730} = \frac{8\sqrt{2}}{1730} \approx 0.06655 \text{ mm}$$

$$\text{DOF} = \frac{2(0.06655 \text{ mm})(50 \text{ mm})^2}{16 \left(\frac{50 \text{ mm}}{16}\right)^2} \approx 2.1296 \text{ mm}$$

Eqn-5 shows us that our DOF is 2.1296mm. This means we will place the target at 5cm, 5.05cm, and 5.1cm away from the ThorLabs lens. Take note that the circle of confusion is calculated using the Zeiss formula since the camera used does not have a listed circle of confusion.

As stated for our purposes, we will use the USAF target instead of fluorescent beads as used in [6]. The purpose will be to show that we can try to estimate the PSF for a target that has an unknown illumination pattern, unlike the fluorescent beads. We hope to show that we can use the given algorithm to identify speckles on the target and use it for various diffuser stages to obtain a PSF at varying defocus distances.

D. Algorithm Breakdown

1) *Simulation:* The aim here is to simulate speckles and the PSF of the optical system by modeling the light as it propagates through various stages in the optical setup. The simulated speckles will be used for estimating the experimental PSF and the experiment PSF will be used to cross-validate the estimated experimental PSF. The method used for simulating speckles and PSF is described in more detail in chapters 5 and 6 of *Introduction to Fourier Optics* by Goodman [1].

$$\text{quad_phase}(X, Y, f, \lambda) = e^{-j \cdot \frac{(2\pi/\lambda) \cdot Z}{2 \cdot f} \cdot (X^2 + Y^2)}$$

(6)

$$\text{aperture_circ}(X, Y, r) = (\sqrt{X^2 + Y^2} < r)$$

(7)

$$\text{fresnel_prop}(X, Y, Z, \lambda) = e^{j \cdot \frac{\pi}{\lambda} \cdot \frac{(x^2 + y^2)}{Z}}$$

(8)

$$\text{uniform_dist_random_phase}(X, Y) = e^{j \cdot \phi_d(X, Y)}$$

(9)

$$MTF = \mathcal{F}(\text{Exit Pupil} \cdot \text{Random Phase})\mathcal{F}(\text{Fresnel Prop})$$

(10)

$$PSF = |\mathcal{F}^{-1}(MTF)|^2$$

(11)

We start by obtaining the parameters such as the light wavelength (680nm), source after diffuser radius (2.5mm), and diffuser-to-object distance (35cm). The PSF is then calculated using the inverse Fourier transform of the MTF, and the resulting speckles are normalized.

Once we have the simulated speckles we move onto simulating the PSF for different distances within a two-lens optical system. It involves the Fresnel propagation of each stage, exit pupil calculations, and lens propagations. The MTFs for each stage are computed using Fourier transforms, and the final PSF is obtained by taking the inverse Fourier transform of the product of these MTFs. The resulting PSFs are normalized and returned for analysis. Fig-3 shows the optical path from the USAF target to the camera sensor and highlights the MTF and PSF at each stage.

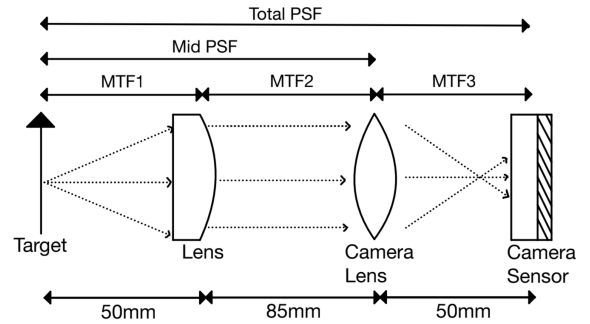


Fig. 3: Optical Path of USAF Target to Camera Sensor at best focus

We then use the following given MTF expressions to formulate the PSFs as follows. Starting at the first stage:

$$MTF_1 = \mathcal{F}(\text{Exit Pupil} \cdot \text{1st Lens} \cdot \text{Propagation from target to lens})$$

(12)

For the second stage, assuming no pupil, the MTF is given by:

$$MTF_2 = \mathcal{F}(\text{Propagation from 1st lens to camera lens})$$

(13)

The PSF at the middle stage is calculated as the inverse Fourier transform of the product of the MTFs:

$$PSF_{mid} = \mathcal{F}^{-1}(MTF_1 \cdot MTF_2)$$

(14)

Post-normalization, we move to the front of the camera lens and simulate the propagation through the camera lens:

$$\text{Light Wave} = PSF_{mid} \cdot (\text{Propagation through camera lens}) \quad (15)$$

$$MTF_3 = \mathcal{F}(\text{Propagation from camera lens to sensor}) \quad (16)$$

The total PSF is then obtained as the inverse Fourier transform of the product of the remaining MTFs:

$$PSF_{tot} = \mathcal{F}^{-1}(\mathcal{F}(\text{Light Wave}) \cdot MTF_3) \quad (17)$$

These simulations are then used to generate computer simulations of our optical setup which is then used as a prior knowledge token in the estimation of the PSF based on speckle illumination.

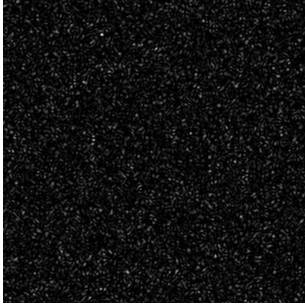


Fig. 4: Simulated Speckles described from Goodman [3] for a distance of 50.5mm

2) *Speckle Extraction*: The PSF recovery method requires that speckles be detected on the simulated and captured experimental data. This is accomplished by detecting areas of the image with relatively higher intensity. In this work, this is performed by using the Laplacian of Gaussian method which is implemented in the *scikit-image* feature detection package [10]. The σ_{min} and σ_{max} values are chosen manually so that only a single speckle is detected per window and the window sizes are the same, the threshold value should be set sufficiently high so that speckles are detected and not extraneous objects in the background.

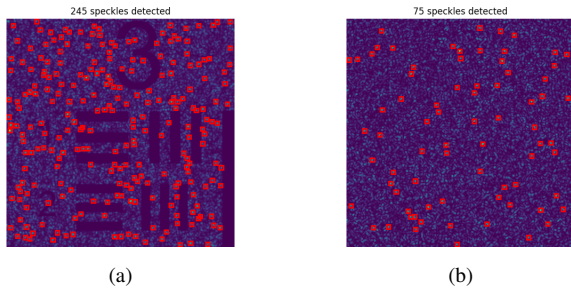


Fig. 5: Speckle Extraction for (5a) noisy image with applied PSF and (5b) simulated speckle pattern

3) *PSF Estimate/Recovery*: As described in Meitav et. al [6], recovering the speckles becomes an error minimization problem:

$$\epsilon = E\{|P - G \cdot I\}^2 \quad (18)$$

with solution:

$$\mathcal{F}^{-1}(G \cdot I) = \mathcal{F}^{-1} \left(I \cdot \frac{1}{S_c} \frac{|S_c|^2}{|S_c|^2 + \frac{1}{c^2} \frac{|N'|^2}{|P|^2}} \right) \quad (19)$$

where:

- S_c is the Fourier transform of the computer simulation of the average speckle
- I is the Fourier transform of the averaged speckle from experimental data
- $\frac{1}{c^2} \frac{|N'|^2}{|P|^2}$ is a term that is dependant on the noise distribution, in our work this term was set equal to the inverse SNR.

This solution arises from the observation that for non-overlapping speckles we can model the average speckles as:

$$\frac{\bar{i}_l}{c} = p \otimes \left(\frac{k}{c} \bar{s}_l \right) + \frac{\bar{n}_l}{c} \quad (20)$$

- p is the PSF
- \bar{o}_l is the average of the fluroescent densities, this is averaged into a constant factor.
- \bar{s}_l is the average speckle intensity.
- \bar{n}_l is the average noise function.
- k is the average of the objects fluroescent density (constant in our case).
- c is a normalization factor so that $\frac{\bar{i}_l}{c}$ has total intensity of one.

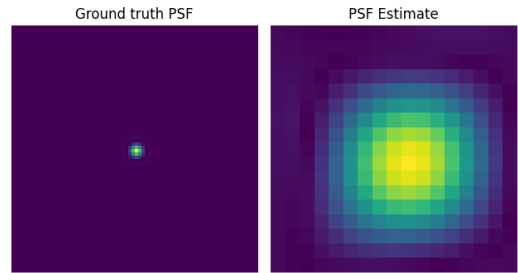


Fig. 6: PSF Estimate for best focus vs theoretical PSF retrieved from simulation data

IV. EXPERIMENTAL RESULTS

Based on the optical setup in Fig-3 we captured sets of images for 3 focal distances. For each focal distance, we changed the angle of the rotation stage to apply different phase changes for the diffuser. The purpose of this was to obtain

different speckle patterns for the same distance and see if we could recover the PSF across all the images.

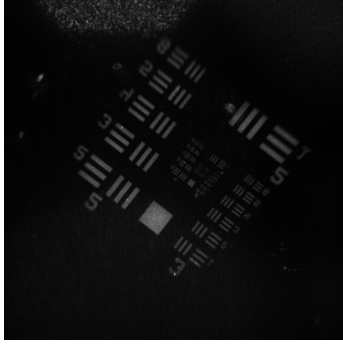


Fig. 7: Data captured from USAF target at best focus (50mm)

From Fig-7 we can observe that the speckle pattern illuminated on the USAF target is very small. These points are too small for the given speckle extraction algorithm to detect. Recall that we want to identify singular speckles per window and so the current data set shows us our first limitation, speckle size. This leads us to use synthetic data developed from the specifications of the optical setup provided.

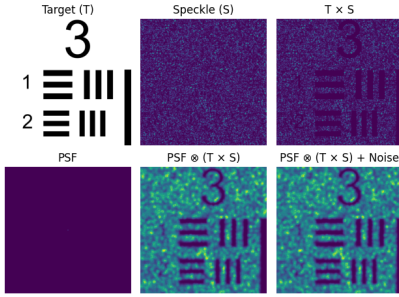


Fig. 8: Synthetic Data Pipeline to represent the speckle pattern illuminated on the USAF target with applied noise (all values are derived from specifications of the optical parts)

Based on these figures and simulation data we can move forward to estimating the PSFs for varying focal distances and comparing them to their theoretical results. To verify the performance of the proposed algorithm, we will conduct 2 tests: measurement of estimated PSF vs theoretical PSF for varying distances with fixed noise (50 dB) and measurement of estimated PSF vs theoretical PSF for varying noises at a best focal distance (50mm). Using these data results we can then do a qualitative and quantitative analysis.

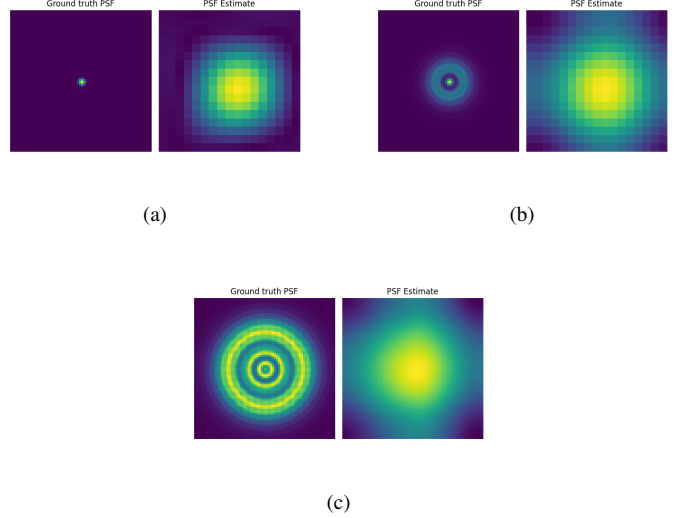


Fig. 9: PSF Intensity Comparisons for (9a) best focus at 50mm, (9b) mid focus at 50.5mm, (9c) worst focus at 51mm.

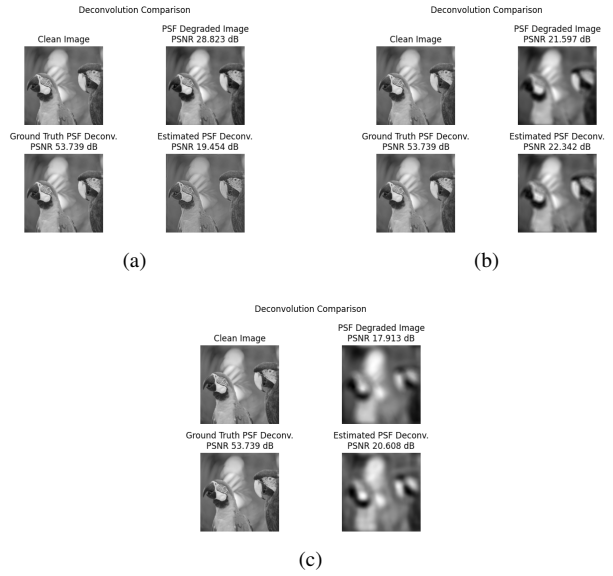


Fig. 10: Test 1: (10a) Deconvolution comparison at best focus (50mm); (10b) Deconvolution comparison at mid focus (50.5mm); (10c) Deconvolution comparison at worst focus (51mm)

SNR applied to image (dB)	50	20	10	6.699
PSNR post deconvolution (dB)	25.696	25.694	25.691	25.691

TABLE II: Test 2: PSNR of deconvoluted images using the estimated PSF at best focus (50mm) for varying noise levels

V. DISCUSSION

As briefly stated earlier, Fig-5a shows the data captured on the USAF target at best focus. If seen closely, we can identify

speckles illuminated on the target from the source to be about the size of a pixel. As we vary the distance the size may get larger but since it is very small to detect the effect imprinted by the PSF we are unable to use these captured images for our PSF estimation. To overcome this hurdle we can develop sets of synthetic data that mimic what our optical setup will have. The creation of simulated experimental data is achieved by the pipeline outlined in Fig-8. We start by capturing the target and simulating the speckle pattern of our optical setup. We then multiply these values to mimic the speckle illumination on the target and convolute it with the theoretical PSF for the varying focal distances. Finally, we can add some photon shot noise that represents the noise added by the sCMOS camera. The final image in Fig-8 will then be used as the replacement of the experimental data to estimate the PSF.

It can be seen in Fig-9 that for varying focal distances the simulated PSF of the illumination path starts to grow and develop more airy disks. This result makes sense as the focal length increases, the convergence of light rays becomes more gradual resulting in larger airy disks. Note the airy disk is a pattern that occurs due to diffraction and can be related to the aperture of the optical system. From our results, we can see that at best focus (Fig-9a) the intensity of the PSF is mainly around the center of the disk and then it starts to spread out and quickly decays away. The estimated PSF shows a similar pattern and as we increase the focal distance the estimated PSF becomes larger and smoother (Fig-9c) which explains the effects of the airy disk pattern.

The performance of the algorithm is strongly dependent on the accuracy of speckle extraction, this can be seen by examining equation (20). If single speckles are not distinguishable then the algorithm will have poor performance. As seen in Fig-10, we see that at the best focus, the PSF recovery performs worse than expected, at mid-focus, it performs better and at the worst focus it performs worse. At best focus the speckles are small so it is difficult to detect speckles due to the speckle being smaller than the detection threshold. At mid-focus the performance does slightly improve as the speckles are larger and easier to detect and at worse focus the speckles are overlapping and hard to distinguish. Table-II shows that at best focus and varying noise levels, the recovered PSF is roughly the same, this is because when averaging the speckles, the noise gets averaged out.

VI. CONCLUSION

In our experiments, we found this algorithm did not perform as well as expected and the main reason for this was the speckle extraction algorithm. Future improvements would be different experimental setups for larger speckle sizes and using various magnification ratios to see if that would make speckles easier to detect. Note this may lead to some modification of the algorithm to compensate for the change in magnification but based on the magnification ratio we can add it to the speckles extraction method. Using more accurate methods speckle extraction would also be a path to explore.

VII. ACKNOWLEDGEMENTS

We would like to thank Jie Jao for helping us with the optical setup and capturing the experimental data, Dylan Dao for helping us break down the components of the algorithm and guiding us through the simulation setup, Dr. Ofer Levi for providing technical guidance with the optical setup, and Dr. David Lindell for mentoring and providing us with feedback throughout the project.

REFERENCES

- [1] Joseph W. Goodman. *Introduction to Fourier Optics*. W. H. Freeman and Company, 2017. Chap. 5, 6. ISBN: 9781319119164.
- [2] Joseph W. Goodman. *Speckle Phenomena in Optics: Theory and Applications, Second Edition*. SPIE, 2020. Chap. 1, pp. 1–6. DOI: 10.1117/3.2548484.ch1.
- [3] Joseph W. Goodman. *Speckle Phenomena in Optics: Theory and Applications, Second Edition*. SPIE, 2020. Chap. 5, pp. 129–174. DOI: 10.1117/3.2548484.ch5.
- [4] B Hwang, R Piestun, and K Irsch. “Non-Isoplanatic PSF and Image Estimation Using Speckle Illumination”. In: (2023).
- [5] B Hwang et al. “Imaging through Random Media Using Coherent Averaging”. In: *Laser & Photonics Reviews* 17.3 (2023), p. 2200673. DOI: 10.1002/lpor.202200673.
- [6] N Meitav, EN Ribak, and S Shoham. “Point spread function estimation from projected speckle illumination”. In: *Light: Science & Applications* 5.3 (Mar. 2016), e16048. DOI: 10.1038/lsa.2016.48.
- [7] E Premillieu et al. “Blind speckle illumination for aberration correction”. In: *Frontiers in Optics*. Optica Publishing Group. Nov. 2021, FM5C.6. DOI: 10.1364/FIO.2021.FM5C.6.
- [8] Warren J. Smith. *Modern Optical Engineering*. 4th. New York, NY: McGraw-Hill Education, 2008. Chap. 15.8, pp. 385–390.
- [9] V. V. Tuchin. *Dictionary of Biomedical Optics and Biophotonics*. Vol. PM217. Apr. 2012, pp. 1–595. DOI: 10.1117/PM217.ch1.
- [10] Stéfan van der Walt et al. “scikit-image: image processing in Python”. In: *PeerJ* 2 (June 2014), e453. ISSN: 2167-8359. DOI: 10.7717/peerj.453. URL: <https://doi.org/10.7717/peerj.453>.